Systematic study for a comprehensive evaluation of PPSU modified with ZnO for ultrafiltration membranes: morphological characteristics and performance

Ali N. Shawket[a], Nisreen S. Ali[a], Qusay F. Alsalhy[b],*

[a]Materials Engineering Department, college of Engineering, Al-Mustansiriya University, Baghdad, Iraq,
emails: alaoi.we1994@gmail.com (A.N. Shawket), nisreensabah@uomustansiriyah.edu.iq (N.S. Ali)
[b]Membrane Technology Research Unit, Chemical Engineering Department, University of Technology-Iraq,
Alsinaa Street 52, 10066 Baghdad, Iraq, email: qusay_alsalhy@yahoo.com/qusay.f.abdulhameed@uotechnology.edu.iq

ABSTRACT

In the current work, zinc oxide nanoparticles (ZnO-NPs) were impregnated within poly(phenyl sulfone) (PPSU) membranes to prepare ultrafiltration nanocomposite membranes with disparate ZnO-NPs 0, 0.3, 0.5, 1 and 1.5 wt.%. A series of characterization measurement tools were harnessed to define membrane characteristics, including contact angle test, scanning electron microscopy, atomic force microscopy and mechanical test. Membranes fluxes and separation trade-off were assessed via an ultrafiltration lab scale testing apparatus. Results showcased that all the prepared ZnO-PPSU membranes have significantly improved morphological properties and performance compared with the nascent PPSU membrane. The optimum flux of (92 L/h·m²) and rejection of about (91%) was obtained by the membrane fabricated with 1 wt.% ZnO-NPs along with no significant deviation in their rejections. Besides, membrane porosity has significantly decreased with increasing of ZnO-NPs content in the PPSU polymeric matrix. Nonetheless, increasing ZnO-NPs concentration in the dope solution have weakened the mechanical properties of the nanocomposite membranes. Based on the obtained results in this work, the nanocomposite membrane modified with ZnO could give a good opportunities for wide range of UF applications especially for membrane bioreactor.

Keywords: Mixed matrix membrane; Membranes modification; Inorganic nanoparticles; Poly(phenyl sulfone); ZnO; Membrane performance

1. Introduction

As a novel class of materials, nanocomposite membranes have attracted wealthy research interest in recent few past years. Merging the characteristics of both nanomaterials and polymers are believed to impart extraordinary properties to the resultant nanocomposite membranes [1]. In this context, membranes fouling is a key problematic concern in membrane filtration processes that could diminish the entire performance and raise the operational costs. Therefore, unfavourable and unavoidable phenomena in the meantime must be efficiently controlled for sustaining a prolonged membrane lifespan [2–4]. Limitless nanostructures were harnessed for this purpose as a mean of hydrophilic modification [5–8]. However, zero-dimension metal oxide nanoparticles (e.g., ZnO) have demonstrated a great potential for membranes modification through revising the membrane surface aiming to alleviate membranes fouling.

Among the available membrane-based filtration processes, ultrafiltration (UF) has acquired a high reputation due to its application's versatility. With a pore size ranging from 1–100 nm, UF membranes manifested a remarkable potential to treat a wide spectrum of harsh municipal and industrial wastewaters. Along with performing as a prominent

* Corresponding author.

pretreatment barrier against pathogens and particulates for desalination RO membranes [9]. Several commercially available polymers have been frequently harnessed as UF membranes fabrication materials, for example, polyacrylonitrile, polyethersulfone, polysulfone (PSf), poly(phthalazineone ether sulfone ketone), poly(vinyl butyral) and polyvinylidene fluoride [10]. However, the undesirably hydrophobic nature of these polymers made them prone to inherent fouling during the operations. This ultimately necessitates exceptional solutions for the sustainability and economical feasibility of the intended separation process.

Parallel to the steady evolution in membranes modification, the integration of inorganic nanoparticles within the polymeric matrix has witnessed a stunning research area. One of these extensively produced nanoparticles was ZnO-NPs for multidisciplinary purposes. Aiming to mitigate polymeric membranes fouling issues ZnO-NPs had easily found their way into polymeric membrane applications due to their favourable characteristics, for example, high catalytic activity, antibacterial and hydrophilic nature [11,12]. Balta referred that ZnO possesses fascinating features and could potentially hold the objectives of nanocomposite membranes with greater performance at a lower cost and ultralow concentrations [13]. In other work, ZnO-NPs have demonstrated their potential to enhance the properties of PSf membranes through improving the permeability and fouling by oleic acid [14]. Also, ZnO/PVDF mixed matrix membranes manifested higher rejection against bovine serum albumin solution with lower flux decline [15].

The current work intended to prepare mixed matrix membranes comprising poly(phenyl sulfone) (PPSU) and ZnO-NPs. It is worth mentioning that utilizing ZnO-NPs for the modification of the PPSU UF membrane has not been widely reported in the preceding literature. Herein, a range of ZnO nano additives was blended with the PPSU polymer during the fabrication whereas a full characterization for the nanocomposites and their performance was evaluated. This work introduced a systematic framework for investigating the threshold of ZnO additives within the PPSU matrix and their influence on both morphological and performance characteristics.

2. Experimental

2.1. Materials and reagents

Polyphenylsulfone (PPSU, Radel R-5000) with 50 KDa average Mw was supplied by Solvay Advanced Polymers (Belgium). 1-methyl-2-pyrrolidone (NMP, purity 99.5%) was purchased from Sigma-Aldrich (Germany). Zinc oxide (ZnO) nanoparticles (purity: 99.8% and 10–30 nm diameter) were obtained from Sky Spring Nanomaterial's Inc., USA. PVP-K90 with an average molecular weight of 60,000 and PVP-K30 with an average molecular weight of 40,000 was purchased from DIREVO Industrial Biotechnology and Central Drug House (P) Ltd., respectively.

2.2. Membrane preparation

All mixed matrix membranes were prepared by the classical phase separation method it is called the phase inversion method. Briefly, five loading weights 0, 0.3, 0.5, 1, and 1.5 wt.% of ZnO-NPs were homogeneously dispersed in NMP by a magnetic stirrer for 3 h. Thereafter, 15 wt.% of PPSU was added to the suspension and continuously stirred overnight at 40°C. Following the degassing stage, the dope solution was cast on a glass substrate with 200 μm clearance gap and placed in a water bath for precipitation [16,17]. Finally, nanocomposite membranes were rinsed several times and stored until further use.

2.3. Membrane characterization

The surface and cross-sectional morphology of the control and mixed matrix membranes were imaged via scanning electron microscopy (SEM, ZEISS-EVO MA10). The samples were initially fractured in liquid nitrogen and then coated with a thin layer of gold before the SEM measurements.

Surface topography analysis was carried out utilizing atomic force microscopy (AFM) model AA3000 Scanning Probe Microscope (Angstrom Advanced Inc., USA). AFM is a potent tool to determine the membranes surface parameters, including mean roughness (R_a), mean pore size and pore size distribution from the 2D and 3D tomographic images with the aid of the AFM software program.

The porosity of samples was assessed via the gravimetric analysis, according to the Eq. (1) [18,19]:

$$\varepsilon = \frac{\left(W_1 - W_2\right)}{\left(A \times T \times \rho\right)} \tag{1}$$

where ε: porosity (%), W_1: the weight of wet membrane (g), W_2: the weight of dry membrane (g), A: effective area of membrane (cm^2), T: membrane thickness (μm), ϱ: water density (0.998 g/cm^3 at 25°C). Before conducting the measurements, membrane samples of nascent and modified PPUS membranes were firstly soaked in deionized water for 24 h at room temperature. The membranes surface were then wiped out from excessive water and the weight was measured again. The average porosity of the membranes was estimated by performing three triplicates for each sample.

Hydrophilicity/hydrophobicity measurements were conducted utilizing the common sessile drop method. An optical instrument (Insite IG Model 35/35L, USA 2013), was employed to capture the contact angle between the DI water droplet and membrane surface which then measured by the instrument software. An average of at least three measurements for three different samples were used during the calculations.

Mechanical properties of the modified membranes were evaluated aiming to investigate the effect of nano additive wt.% on the membranes. The tensile strength and elongation of the prepared membranes were assessed using a tensile tester (Tinius Olsen H50KT Universal Tester, UK). Results obtained by taking the average of three different samples for the same membrane having dimensions of (100 mm × 20 mm).

The UF nanocomposite membranes pure water permeation and solute separation characteristics were assessed under a crossflow filtration mode. The UF testing rig was equipped with an effective membrane area of 0.0014 m^2.

Measurements were conducted under the effect of constant adjustable operating pressures at room temperature. For the UF membranes separation evaluation, two feed solutions have been employed with unlike molecular weight cut-off; PVP-K30 and PVP-K90. Initially, membranes were compacted at 4 bar for 20 min prior to the filtration test and then lowered to the required operating pressure. The pure water permeability was calculated as follows:

$$\text{Pure Water Permeability} \left(\text{PWP} \right) = \frac{\text{Volume}}{\text{Time} \times \text{Area}} \left(\text{L/m}^2\text{h} \right) \quad (2)$$

The rejection tests were determined using a 1,000 ppm aqueous solution of PVP-K90. The concentration of PVP in the permeate was found using UV-spectrophotometer (Shimadzu-UV160 A, Japan), at 212 nm wavelength. The retention efficiency (*R* %) was calculated based on Eq. (2):

$$\left(R\% \right) = \left(1 - \frac{C_p}{C_f} \right) \times 100\% \quad (3)$$

where C_p and C_f are permeate and feed concentrations of PVP, respectively.

3. Results and discussion

3.1. Influence of ZnO-NPs on the structure of the prepared membrane

3.1.1. Scanning electron microscopy and energy-dispersive X-ray spectroscopy

The morphological changes induced by impregnating ZnO-NPs into the membranes polymeric matrix are illustrated in Figs. 1 and 2, for the top surface and cross-section, respectively. As shown in the surface images (Fig. 1A–E), the ZnO-NPs could be seen on the surface of nanocomposite membranes and their concentration on the surface increased upon increasing the loading ratio in the dope solution as depicted in the top right corner images of energy-dispersive X-ray spectroscopy (EDS). This confirmed the successful incorporation of the nanoparticles at the required composition within the polymeric matrix where part of the ZnO-NPs moved to the surface during the phase separation process. In the meantime, small aggregates were detected at the higher (1–1.5 wt.%) ratio of nanomaterials used. Meanwhile, the number of visible pores seemed to be influenced by increasing the ZnO loading in the matrix nanocomposites which will be discussed later in the subsequent sections. Similar observations were detected in the preceding literature and concluded the addition of ZnO-NPs can considerably enhance the porosity of the membrane up to a specific loading ratio. Also, a further amount of ZnO was realized to impart a slightly adverse influence on the entire porous structure of the membrane by producing denser structure and trivial lower porosity nanocomposite membranes [13,20].

For the cross-sectional analyses, a clear sponge-like structure was observed in the nascent PPSU membrane along with some small evenly distributed microvoids throughout the cross-section of the membrane (Fig. 2A). Following the addition of 0.3 wt.% ZnO-NPs in the PPSU matrix, a well-formed finger-like structure from the top to the bottom was observed as depicted in Fig. 2B. This finger-like structure was also noticed when utilizing a higher nano additives rate (0.5 wt.%) but with a narrower structure (Fig. 2C). Further increase in the ZnO content has induced a denser sponge structure to be formed especially at the bottom of the membranes whereas a denser skin layer has been seen at the top. As could be seen in Fig. 2D, rising the ratio of ZnO-NPs content from 0.5 to 1 wt.% have induced a more sponge-like layer formation along with a wider finger like-structure and least number. At 1.5 wt.% ZnO-NPs, nearly half of the cross-section has been turned into a sponge-like structure near the bottom while the remaining finger-like structure was small and short with a larger number of fingers (Fig. 2E). This could be ascribed to the enhanced viscosity of the dope solution at higher NPs ratios. Indeed, suppressed the solvent-nonsolvent exchange rate and resulted in a denser structure and less pore formation. These findings were generally agreed with a previous work conducted by Yang et al. [21].

3.1.2. Atomic force microscopy

Surface roughness was considered a critical parameter for predicting the antifouling characteristics of membranes. Membranes with a smoother surface were believed to impart better fouling resistance while rough membrane surface could be more prone to rapid fouling [11]. The 2D and 3D surface topography images of the neat and ZnO-NPs modified membranes are depicted in Fig. 3. In these images, the dark regions represented the lowest points (valleys) whereas the bright regions indicated the highest points (peaks) [22,23]. All membranes showcased a smooth surface, which is the intrinsic surface characteristic correlating with PPSU membranes. Clearly, the structure of the neat PPSU membrane surface comprised of thin long nodular aggregates (Fig. 3A). These nodular aggregates have been separated and became needle-like aggregate when adding 0.3 ZnO-NPs, as shown in Fig. 3B. In the meantime, adding 0.5 wt.% ZnO-NPs, the nodules merged and turned into long wide aggregates, as illustrated in Fig. 3C. Greater wide nodules aggregates with round edges and soft appearance were observed at ZnO-NPs up to 1 and 1.5 wt.% (Fig. 3D and E). There was no clear correlation was observed between the roughness parameters and the NPs impregnation into the polymeric matrix. The mean value of the surface relative to the centre plane (R_a) was found to at its lower magnitude (2.4 nm) for the 0.5 wt.% and highest value (7.4 nm) for the 1 wt.% nano additives. The influence of ZnO-NPs addition on the mean roughness (R_a), the root mean square of Z-values (R_{ms}), and maximum roughness (R_{max}) (vertical distance between the highest peaks and the lowest valleys) are listed in Table 1.

3.1.3. Pore size, pore size distribution, porosity and thickness

The influence of ZnO-NPs on PPSU membrane pore size and their distribution are illustrated in Figs. 4 and 5, respectively. A clear declining correlation is revealed by the figure between the NPs ratio and pore size of the membranes. As could be seen, the pore size of the PPSU membranes has
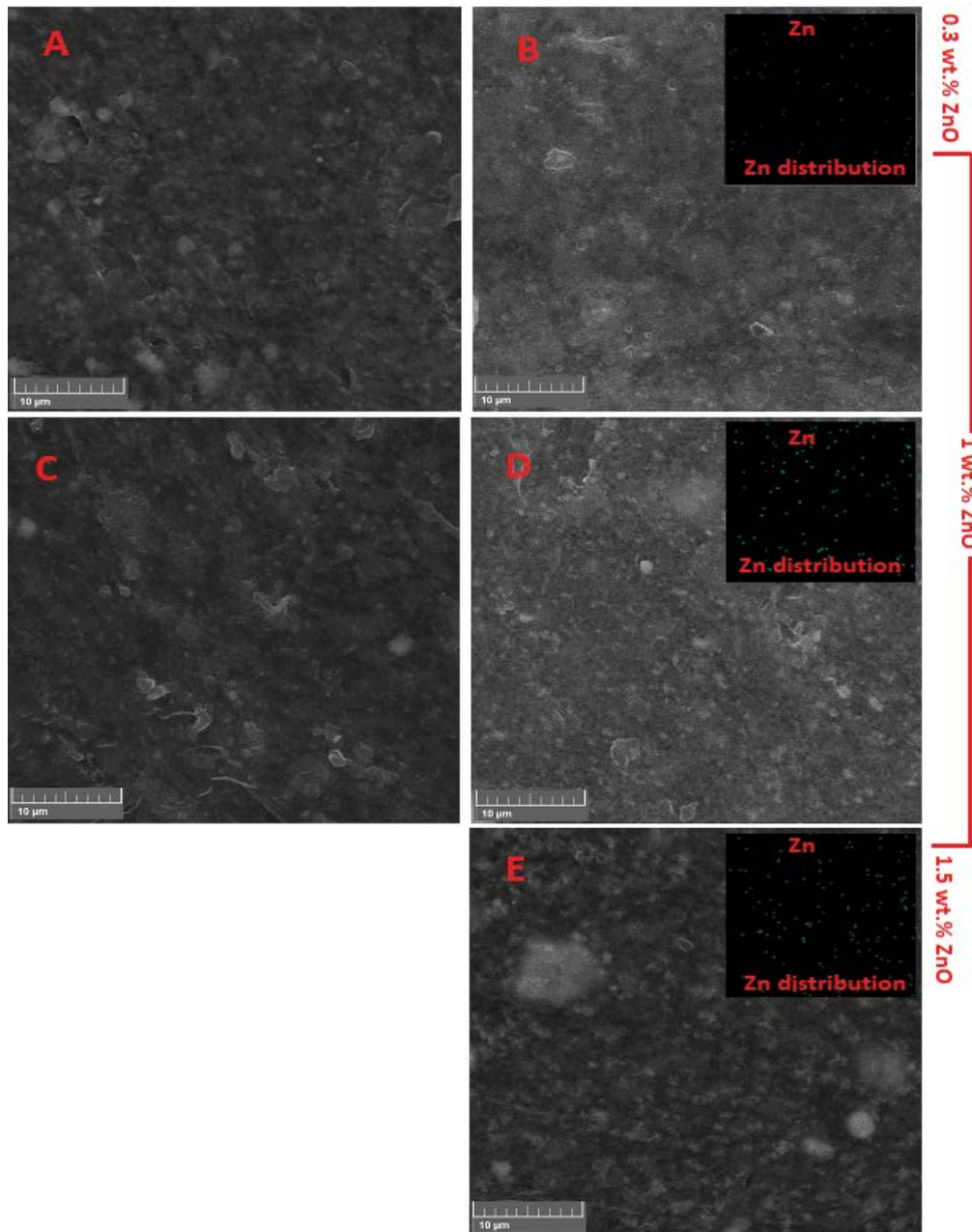
Fig. 1. Top surface SEM images and ZnO distribution (EDS analysis) of the UF membranes at various ZnO loading ratio; (A) neat, (B) 0.3%, (C) 0.5%, (D) 1% and (E) 1.5 wt.%.

steadily decreased from 137 nm for the neat PPSU membrane to about 131 nm with increasing the ZnO-NPs content to 0.3 wt.%. Further increase in nano-additive contents has induced an additional decline to about 118, 116 and 102 nm for the 0.5, 1 and 1.5 wt.%, respectively.

These results have agreed with others reported by Alsalhy et al. [12] who found that the addition of ZnO-NPs into PPSU casting solution (at a concentration up to 0.025 wt.%) could increase the pore size. However, when the additives were higher than 0.025 wt.%, a decrease in the pore size of the membranes have been detected. Similarly, Ahmad et al. [24] indicated that a decreasing trend in

the pore size was observed at high ZnO-NPs concentrations (≥1 wt.%). In this context, the pore size distribution of the mixed matrix membranes is illustrated in Fig. 5. As can be seen, the distribution curves have shifted to the left as the ZnO-NPs weight percent was increased in the casting solution. Additionally, mixed matrix membranes with lower nano additives ratio 0.5 wt.% or lower tended to reveal a sharp cut-off in pore size distribution. These results correlate with the pore size results disclosed earlier in this section. Besides, demonstrated that ZnO wt.% could bestow a significant influence on the permeation characteristics of the modified PPSU membranes.
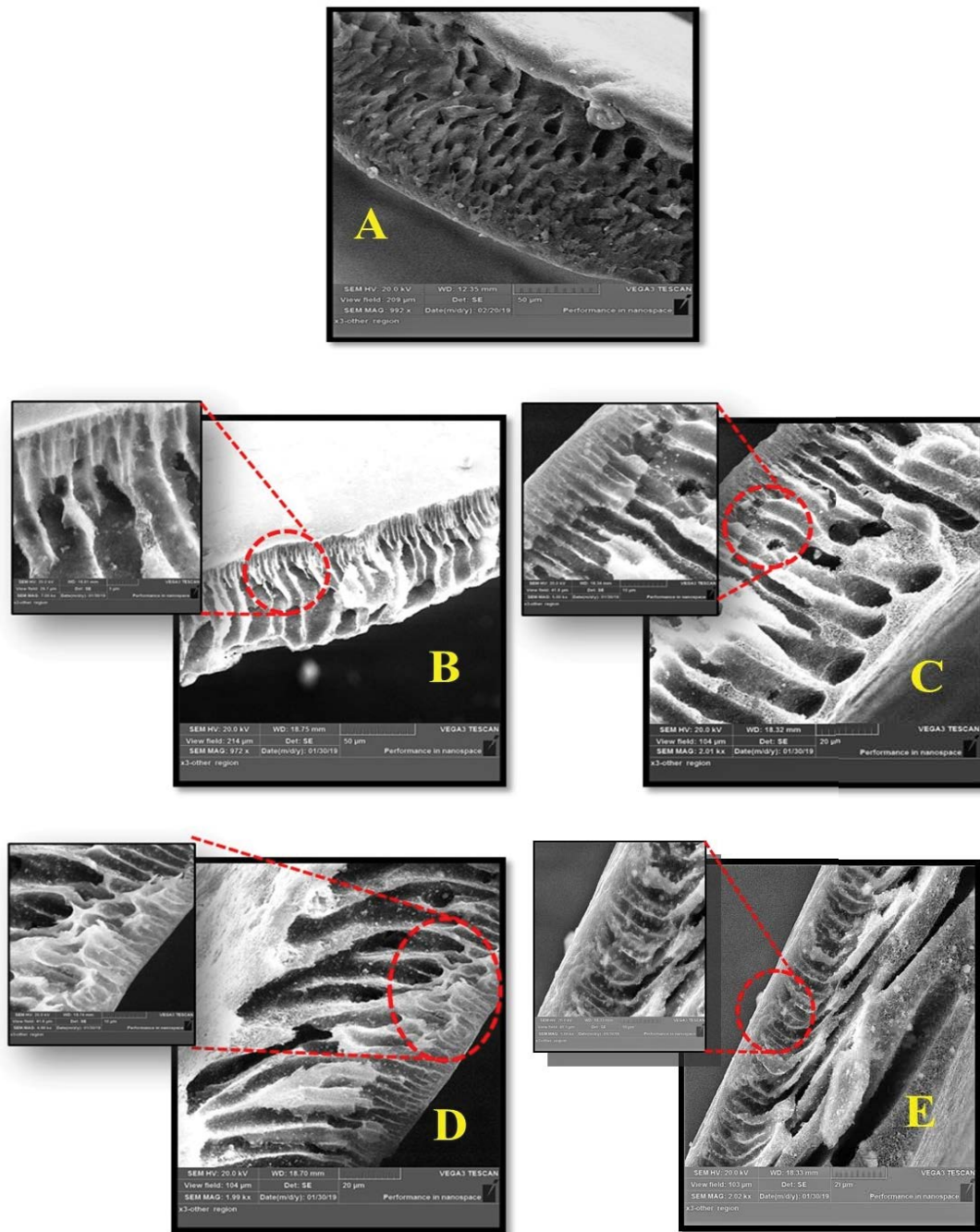
Fig. 2. The cross-sectional SEM images of the PPSU membranes at different ZnO concentrations for (A) neat, (B) 0.3%, (C) 0.5%, (D) 1% and (E) 1.5 wt.%.

Along with that, it is well-known that membrane porosity is another favourable characteristic and is directly related to water flux. The porosity of the membranes modified with the disparate ZnO-NPs composition as illustrated in Fig. 6. As shown, the porosity of the neat PPSU membrane was determined to be around 0.63. However, incorporating 0.3 wt.% ZnO-NPs showcased a slight increase to about 0.64 whereas it was found to be slightly higher (0.65) when the ratio of the additive was 0.5 wt.%. At higher ZnO-NPs loading in the casting solution, a rapidly decreasing trend in

the porosities was realized and found to be 0.58 and 0.55 for the 1 and 1.5 wt.% nanocomposite membranes, respectively. It is worth mentioning here that any membrane porosity could be subjected to the interplay between the hydrophilic characteristics and dope solution viscosity. More likely in this work, the denser structure observed following incorporating high loading content of ZnO (≥ 1 wt.%) have induced the lower porosities. These results were in good agreement with the preceding literature [14,25]. Moreover, it was noticed that there was a significant variation in the
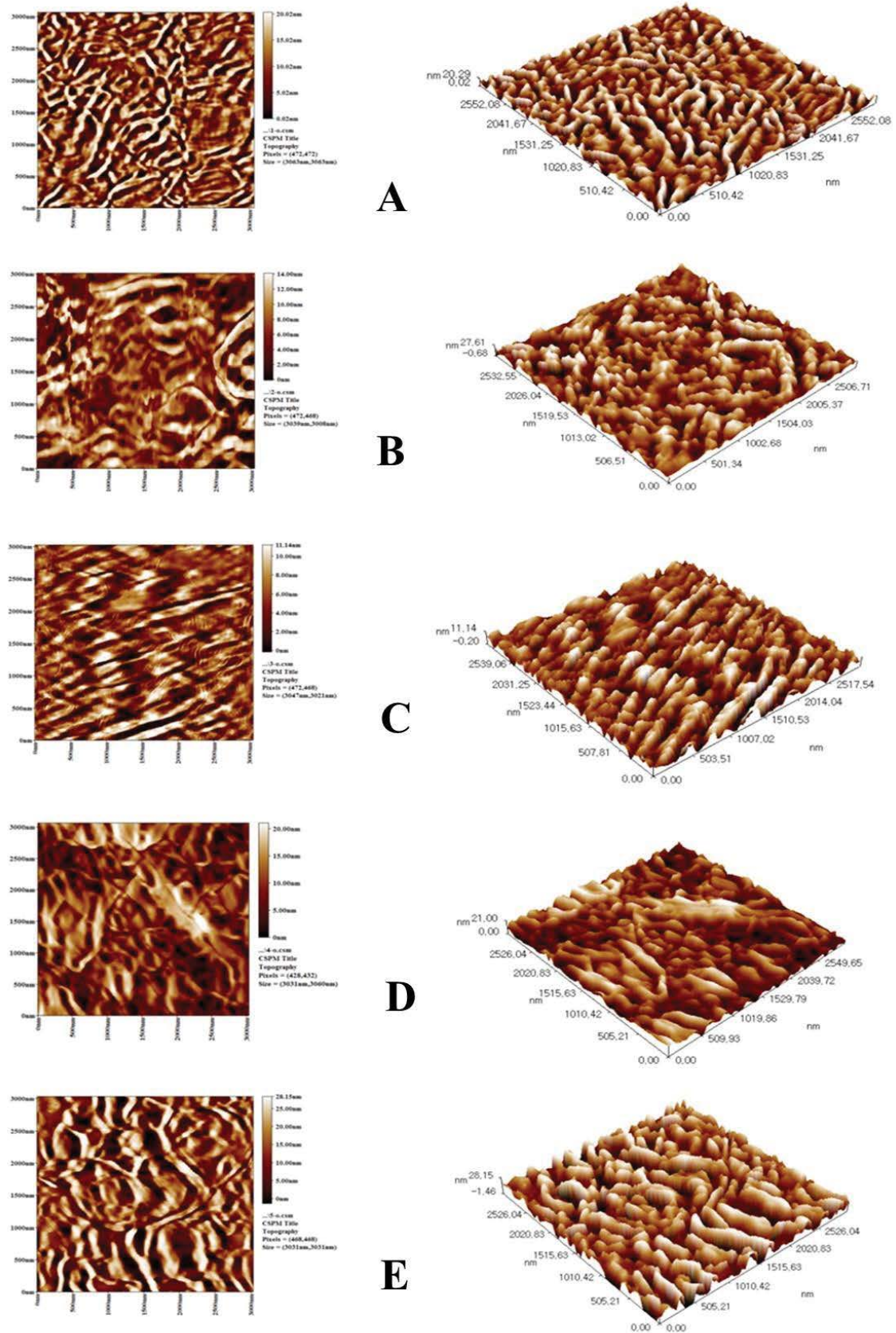
Fig. 3. Three-dimensional AFM images of the PPSU flat sheet membranes at different ZnO concentrations: (A) neat, (B) 0.3%, (C) 0.5%, (D) 1% and (E) 1.5 wt.%.

Table 1
Roughness parameters of the membranes

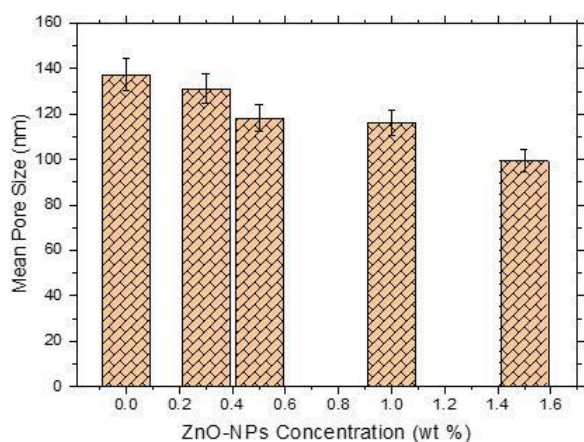| ZnO conc. (wt.%)	Average roughness (R_a) (nm)	Root mean square of Z-values (R_{ms}) (nm)	Max. roughness (R_{max}) (nm)
0	5.07	5.85	17.6
0.3	6.05	7.14	22.3
0.5	2.4	2.89	8.34
1	4.22	5.01	15.3
1.5	7.4	8.55	25.7

Fig. 4. Effect of different concentration of ZnO-NPs on the mean pore size of PPSU membrane.

thickness of the modified membranes compared to the neat PPSU membrane. As disclosed in the figure, a thickness of about 135 micron was observed for control membranes while it was ranging between 57–58 μm for all nanocomposite membranes. This phenomenon is maybe due to the effect of hydrophilic character of the ZnO-NPs resulted in acceleration of the water-solvent exchange rate during the fabrication of PPSU-ZnO membranes, which in turn led to high reduction in the membrane thickness.

3.2. Effect of ZnO-NPs on mechanical properties of PPSU membrane

The membranes robustness can be employed as an indication to predict the entire performance stability under stressed operational conditions. A membrane with a higher mechanical strength encloses a longer membrane lifespan and greater resistance to harsh cleaning [26]. The mechanical properties of fabricated nanocomposite membranes synthesized with different NPs ratio were tested and results are depicted in Fig. 7. Greater values of elongation and tensile strength at break were associated with the nascent PPSU membrane, 6.9 MPa and 14.6% for tensile and elongation at break, respectively. Incorporating ZnO-NPs within the polymeric matrix have caused a gradual decline upon each increment ratio for both values of tensile and elongation at break. Presence of 0.3 wt.% ZnO in the polymeric matrix has

declined the tensile and elongation into 6.3 MPa and 12.98%, respectively. Further increase in the nano additives ratio has continuously decreased the mechanical properties of the nanocomposites. The minimum tensile and elongation was associated with the highest NPs loading ratio (1.5 wt.%) and were reduced by about one-third comparing with the neat membrane. This is due to the presence of NPs result in Nano ZnO particles restricted the space for free movement of the PPSU chain [27]. Similar results were found in the preceding literature [28]. Hong and He [29] reported that incorporating ZnO-NPs into the PVDF membrane could manifest a decline of membrane strengths and its elasticity, thereby leading to a decrease in the tensile strength of membranes and elongation at break value.

3.3. Influence of ZnO on the hydrophilic character

The hydrophilicity of a membranes material could be employed to predict the affinity of that membrane with water passage and antifouling characteristics. Contact angle tests were conducted to assess the impact of ZnO-NPs incorporation on the surface hydrophilicity of the nanocomposite UF membranes. A clear decline in the contact angle values was observed upon impregnating the nanoparticles for all modified UF membranes, as shown in Fig. 8. The higher contact angle value reported in the current work was recorded for the pure PPSU and was 59.4°. the mixed matrix UF membrane prepared with 0.3 wt.% manifests a slight decline for the water contact value by 5° comparing to the bare membrane. Further increase in the amount of ZnO content has induced a further decrease in the value of contact angle. Modified membranes with 0.5, 1 and 1.5 wt.% have disclosed 52.1°, 38.4° and 45.9° contact angles. This indicated the successful incorporation of the nanoparticles within the polymeric matrix which indeed imparted the hydrophilic characteristic of the ZnO on nanocomposite surfaces [12]. It is worth mentioning that membrane prepared with 1.5 wt.% has manifested a slightly higher contact angle (45.9°) comparing to nanocomposite prepared with 1 wt.% ZnO (38.4°). This probably occurred due to agglomeration of the nanoparticles at the highest loading ratio which reduced the NPs surface/volume ratio and eventually reduced the hydrophilic nature of the membrane surface.

3.4. Performance evaluation of the membranes

The pure water permeance and retention characteristics for UF mixed matrix membranes, synthesized with disparate ratios of ZnO-NPs, were compared with that of neat PPSU. Representative organic solutes, PVP-K90 and PVP-K30, have been devoted for evaluation purposes.

As revealed in Fig. 9, a clear increasing trend for pure water flux has been witnessed upon increasing the content of ZnO content in the dope solution. Unsurprisingly, this trend was expected based on the results of improved hydrophilicity, pore size and pore size distribution discussed earlier in this work. It should be noted here that membrane prepared with 1.5 wt.% exhibited the lower water flux (52 LMH) which was still higher than the neat PPSU membrane (27 LMH). The flux of the nanocomposite membrane prepared with 0.3 wt.% ZnO induced an increase in the
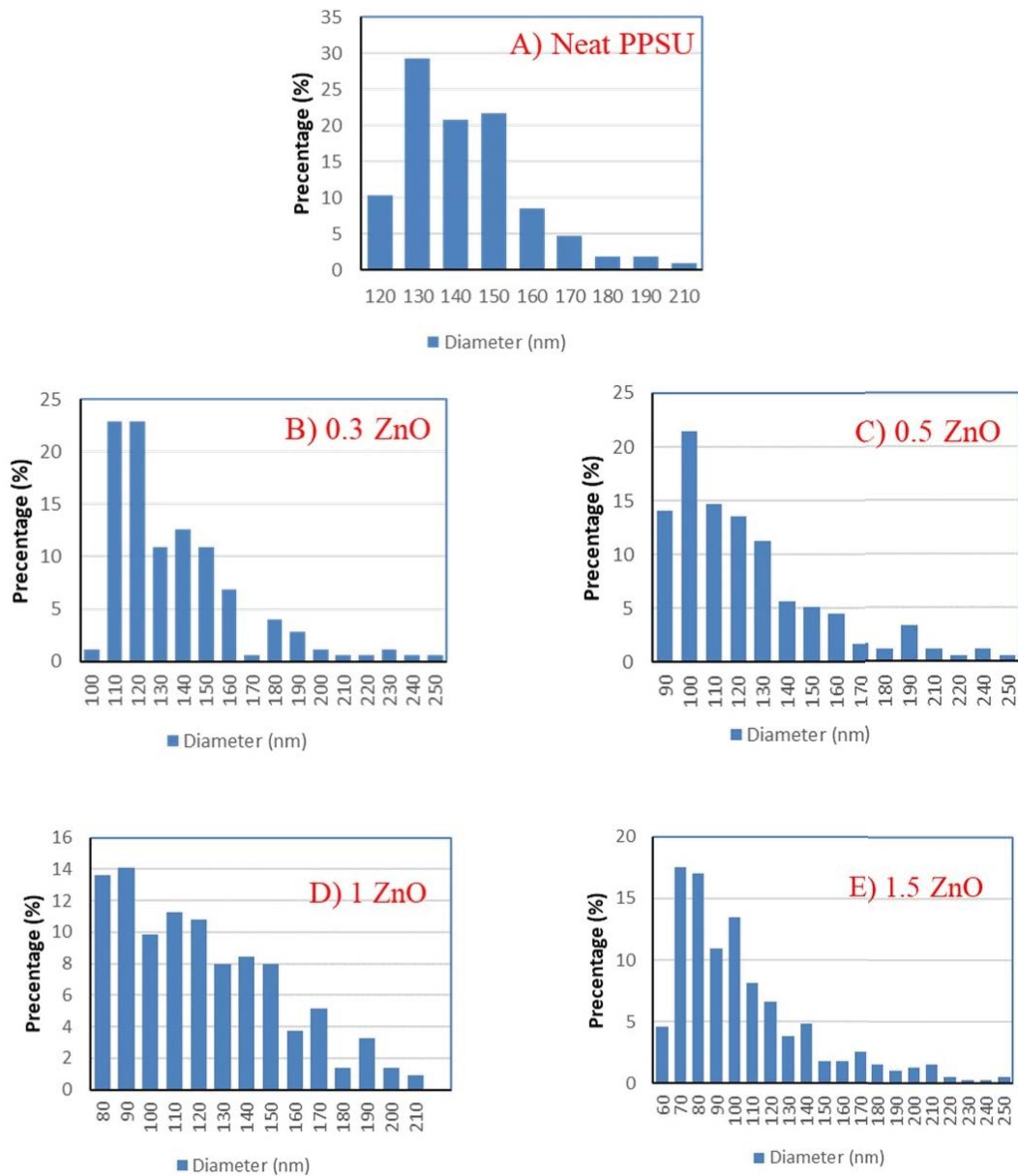
Fig. 5. Pore size distributions the PPSU flat sheet membranes at different ZnO concentrations: (A) neat, (B) 0.3%, (C) 0.5%, (D) 1% and (E) 1.5 wt.%.

PWP to about 48.5 LMH while a further increase to 0.5 and 1 wt.% has manifested about 83 and 92 LMH, respectively. It can be concluded that the PWP of the PPSU membrane has significantly enhanced upon the addition of ZnO-NPs into the casting solution, and maximum flux was obtained for the membrane prepared with 1 wt.% which increased by about 340% compared to that of neat PPSU membrane.

The influence of different ZnO-NPs content in the PPSU casting solution on PPSU membrane separation performance against PVP-K30 and PVP-K90 solutions are illustrated in Fig. 9. In general, it can be noticed that the rejection of neat PPSU membrane to PVP-K90 has not significantly affected by the addition of ZnO-NPs into PPSU casting solution and was higher than 90% for all membranes. This is could be

explained by the large molecular size of PVP-K90 so that the majority of PVP-K90 molecules would be rejected especially since all membranes have a mean pore size ranging between 102 and 137 nm. However, regarding PVP-K30, it can be clearly observed that the rejection values were largely influenced by the increasing of ZnO-NPs content in contrast to PVP-K90. The improvement in rejection was raised from 55% to 65% by only 0.3 wt.% incorporations. Further amounts; 0.5 and 1 wt.% continued to reveal higher retention potentials and achieved about 71% and 83%, respectively. The highest loading (1.5 wt.%) demonstrated the greater separation against PVP-K30. Since all membranes manifested almost different mean pore size but with a comparable pore size distribution. Therefore, a small pore size membrane prepared
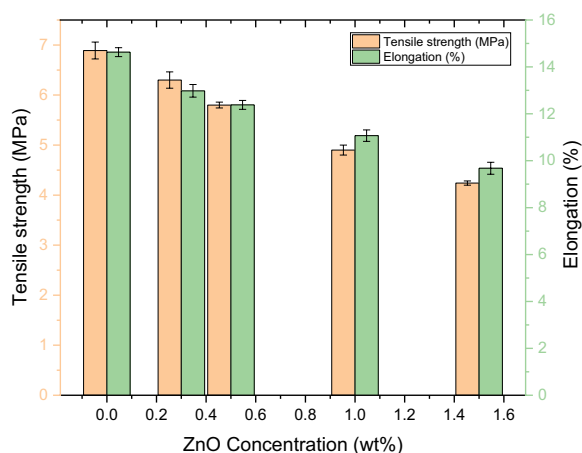
Fig. 7. Effect of ZnO-NPs concentration on tensile strength and elongation of the PPSU membrane.
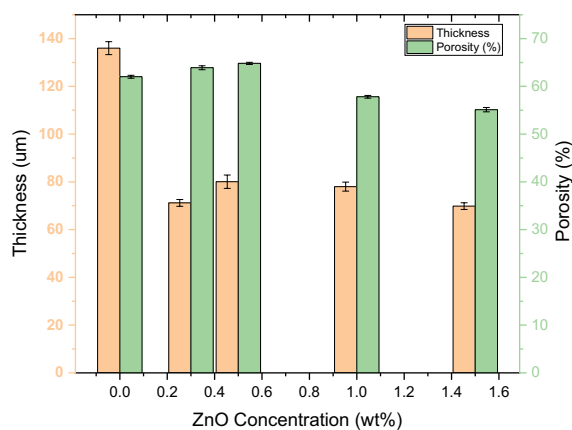

Fig. 6. Effect of different concentrations of ZnO-NPs on PPSU membrane thickness and porosity.

with 1.5 wt.% has achieved a much higher retention value (91%) comparing with other nanocomposite and control membrane.

3.5. Comparative study

Zinc oxide nanoparticles (ZnO-NPs) were impregnated within poly (phenyl sulfone) (PPSU) membranes to prepare ultrafiltration nanocomposite membranes with disparate ZnO-NPs 0, 0.3, 0.5, 1 and 1.5 wt.%. This study was deal with the removal of different type of pollutant. Table 2 shows the comparison between this study and others for different types of membrane used for removel of different types of
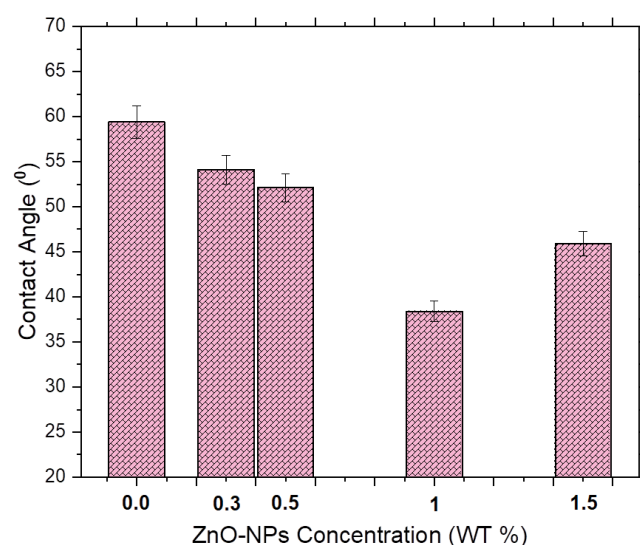
Fig. 8. Contact angles measured for neat PPSU and nanocomposite membranes prepared with different ZnO nanoparticle contents.

Table 2
Comparison between this study and other studies presented in the literature using different base-polymers as a membrane material and ZnO as nanoparticles

Membrane		PWP and permeability	Rejection (%)	References
Polymer	Additive			
Polyethersulfone (PES) (25, 27, 30 and 32 wt.%)	ZnO nanoparticle (0.035–0.750, 1, 2 and 4 wt.%).	At 27 wt.% of PES ZnO 1% = 60 (L/h/ m^{-2}·bar) and 2% = 60 (L/h/m^{-2}·bar)	Methylene blue 5 mg/L Dye PES/ZnO 0.125 ZnO wt.% = 95	[30]
Polyvinyl alcohol (PVA) and polysulfone (PSf) 100:1	ZnO nanoparticles (1, 2, 3, and 4 wt.%)	25.45 (10^{-11} m/s·Pa)	Highly removal efficiency of oleic acid	[31]
Poly(phenyl sulfone) (PPSU) 22 wt.% PPSU	Nano-ZnO 0.01–0.03 wt.%	PWP 0.025 = 107 (L/ m^2/h·bar)	98.6 Fw Direct red 80	[12]
Polyethersulfone (PES) 22%	Graphene oxide – zinc oxide (GO-ZnO) 0.0125%–0.2% GO-ZnO	PWP 0.2% = 13.5 (L/ m^2/h·bar)	28% TOrCs	[32]
Polyvinyl chloride (PVC) 13 wt.%	ZnO nanoparticle 0.1, 0.2, 0.3, and 0.4 g	122.22 (L/h·m^2)	73.65 wt.% COD	[33]
Polyethersulfone (PES) 18 wt.%	ZnO 0.5–1 wt.%	22 (g/cm^2·s)	94% Humic acid	[34]
Polyphenylsulfone (PPSU)	ZnO nanoparticle	287.4 (L/m^2·h)	90	This study

Table 3
Comparison between the performances of membranes prepared by the current work with various membranes found in the literature in terms of membrane properties, total pure water flux, and removal efficiency with different nanoparticles

Membrane material	Nanoparticle and nanosheet	Pore size (nm)	Porosity (%)	Contact angle (°)	Removal efficiency (%)	PWP (L/m²h)	References
PVC (15 wt.%)	MWCNT-g-GO (0.119 wt.%)	259	81.4	13.9	COD: 88.9	254	[16]
15% Polyphenylsulfone and 85% N-methyl-2-pyrrolidinone	0.15% Gum Arabic-graphene	95.57	–	50	88% Sodium alginate	82.11	[35]
Polyphenylsulfone, 1% polyvinyl-pyrrolidone and 81.5%	0.5% Graphene oxide	10.6	80	45	94% BSA and 88% pepsin	171	[36]
18% Polyvinylidene fluoride and 82% N-N-dimethylacetamide	0.1 g/L Oxidized multi-walled carbon nanotubes	8.09	45.33	71.77	81.94% Turbidity, 86.3% color, and 100% TSS of palm oil mill effluent	131.97	[37]
PSf	SiO$_2$-GO/PSf	2.3	–	63	98.3% BSA	360	[38]
PSf/PVP	MXene nanosheets	36	74.4	78.4	98% BSA	306	[39]
PES	ZrO$_2$ (1 wt.%)			52.3	92.7% BSA	83.6	[40]
PES: 21% (2 bar)	SiO$_2$-g-PEI (0.9 wt.%)	27.1	89.9	49	95.4% MBV: 99.99 (100 ppm)	140	[41]
PES (14 wt.%)	SiO$_2$-g-PEI	41.04	82.56%	41	97% BSA	181	[42]
PES (19 wt.%); PVP (1 wt.%)	WO$_{2.89}$ (0.4 g)	74.4	64.2	51.21	44.89% Tinzaparin sodium	54.9	[43]
PES (19 wt.%); PVP (1 wt.%)	WO$_{2.89}$ (0.4 g)	74.4	64.2	51.21	91.56% Congo red (CR) dye	54.9	[44]
PVC (15 wt.%)	TiO$_2$: 1.5 g	77	79.5	62.5°	Oil and grease: 96.3, COD: 79.7, and TSS: 98.8	116	[45]

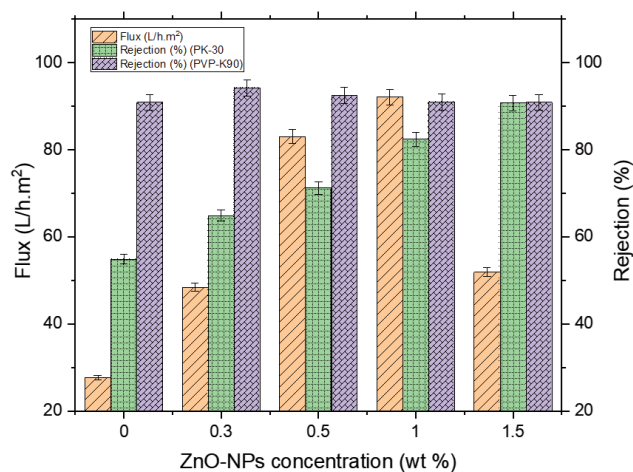BSA: Bovine serum albumin; MBV: mebeverine.

Fig. 9. Effect of ZnO-NPs concentration in PPSU casting solution on pure water permeability, and retention of PVP-K90 and PVP-K30 at operating pressure of 4 bar.

pollutant. Table 3 shows the comparison between the performances of membranes prepared in this study with various membranes found in the literature in terms of membrane properties, total pure water flux, and removal efficiency with different nanoparticles. These two tables show that results of the current study is more reasonable in comparison with that reported in the literature.

4. Conclusion

The following conclusions can be drawn based on this research

- Characterization by SEM for the cross-sectional analysis indicated that the structure of nanocomposites has been changed from the sponge-like structure into a finger-like structure upon the addition of ZnO-NPs. A well-formed finger-like structure from top to bottom was observed at 0.3 wt.% nanocomposite membranes. However, wider structure initiated to unrevealed with further amounts where big microvoids have been formed at the higher ZnO content (1.5 wt.%) in PPSU casting solution.
- Surface topography measurements by AFM disclosed that all membranes had a smooth surface, which is the intrinsic surface characteristic correlating with PPSU membranes. Obviously, there was no clear correlation was observed between the roughness parameters and the NPs impregnation into the polymeric matrix. The mean value of the surface relative to the centre plane (R_a) was found to at its lower magnitude (2.4 nm) for the 0.5 wt.% and highest value (7.4 nm) for the 1 wt.% nanoadditives.
- The contact angle measurements demonstrated higher hydrophilicity values for ZnO modified membranes compared to the neat membrane. Membrane modified with 1 wt.% ZnO-NPs manifested the lowest contact angle (37°) where beyond this content (at 1.5 wt.%), the contact angle starts to increase again due to NPs aggregation inside the membrane structure.
- The PWP of the membranes improved with increasing the ZnO-NPs concentration in the casting solution up to

1 wt.%, as the trend seen in contact angle measurements. Results indicated that PWF has increased by about 340% if compared to that of neat PPSU membrane.
- Separation performance experiments showed a significant enhancement in PVP-K30 separation with the addition of ZnO nanoparticles in the casting solution whereas it was trivial for PVP-K90 removal.
- The porosity of the membranes did not showcase an interesting enhancement upon increasing the ZnO ratio in the casting solution and reach a maximum porosity of (65%) for the nanocomposite membrane prepared with 0.5 wt.% ZnO-NPs in the casting solution.
- Finally, greater values of elongation and tensile strength at break were associated with the nascent PPSU membrane, 6.9 MPa and 14.6% for tensile and elongation at break, respectively. Incorporating ZnO-NPs within the polymeric matrix have caused a gradual decline upon each increment ratio for both values of tensile and elongation at break. The minimum tensile and elongation was associated with the highest NPs loading ratio (1.5 wt.%) and were reduced by about one-third comparing with the neat membrane.
- Based on the obtained results in this work, the nanocomposite membrane modified with ZnO could give a good opportunities for wide range of UF applications especially for membrane bioreactor

Conflicts of interest

The authors of the current work do not have conflict of interest.

References

[1] S. Al Aani, V. Gomez, C.J. Wright, N. Hilal, Fabrication of antibacterial mixed matrix nanocomposite membranes using hybrid nanostructure of silver coated multi-walled carbon nanotubes, Chem. Eng. J., 326 (2017) 721–736.
[2] M.M. Rohani, A.L. Zydney, Protein transport through zwitterionic ultrafiltration membranes, J. Membr. Sci., 397 (2012) 1–8.
[3] Y.-F. Zhao, L.-P. Zhu, Z. Yi, B.-K. Zhu, Y.-Y. Xu, Improving the hydrophilicity and fouling-resistance of polysulfone ultrafiltration membranes via surface zwitterionicalization mediated by polysulfone-based triblock copolymer additive, J. Membr. Sci., 440 (2013) 40–47.
[4] Y.-F. Zhao, L.-P. Zhu, Z. Yi, B.-K. Zhu, Y.-Y. Xu, Zwitterionic hydrogel thin films as antifouling surface layers of polyethersulfone ultrafiltration membranes anchored via reactive copolymer additive, J. Membr. Sci., 470 (2014) 148–158.
[5] L. Yang, B. Tang, P. Wu, UF membrane with highly improved flux by hydrophilic network between graphene oxide and brominated poly(2,6-dimethyl-1,4-phenylene oxide), J. Mater. Chem. A, 2 (2014) 18562–18573.
[6] A.K. Shukla, J. Alam, M.A. Ansari, M. Alhoshan, F.A.A.J.E.S. Ali, P. Research, Antimicrobial and antifouling properties of versatile PPSU/carboxylated GO nanocomposite membrane against gram-positive and gram-negative bacteria and protein, Environ. Sci. Pollut. Res. Int., 25 (2018) 34103–34113.
[7] A.M. Isloor, M.C. Nayak, B. Prabhu, N. Ismail, A. Ismail, A.M.J.R. Asiri, F. Polymers, Novel polyphenylsulfone (PPSU)/ nano tin oxide (SnO₂) mixed matrix ultrafiltration hollow fiber membranes: fabrication, characterization and toxic dyes removal from aqueous solutions, React. Funct. Polym., 139 (2019) 170–180.
[8] S.M. Alardhi, J.M. Alrubaye, T.M. Albayati, Removal of methyl green dye from simulated waste water using hollow fiber ultrafiltration membrane, 2nd International

Scientific Conference of Al-Ayen University (ISCAU-2020), IOP Conf. Ser.: Mater. Sci. Eng., 928 (2020) 052020, doi: 10.1088/1757-899X/928/5/052020.

[9] S. Al Aani, C.J. Wright, N.J.D. Hilal, Investigation of UF membranes fouling and potentials as pre-treatment step in desalination and surface water applications, Desalination, 432 (2018) 115–127.

[10] M. Cheryan, Ultrafiltration and Microfiltration Handbook, CRC Press, Boca Raton, 1998.

[11] S. Liang, K. Xiao, Y. Mo, X. Huang, A novel ZnO nanoparticle blended polyvinylidene fluoride membrane for anti-irreversible fouling, J. Membr. Sci., 394 (2012) 184–192.

[12] Q.F. Alsalhy, J.M. Ali, A.A. Abbas, A. Rashed, B.V. de. Bruggen, S. Balta, Enhancement of poly(phenyl sulfone) membranes with ZnO nanoparticles, Desal. Water Treat., 51 (2013) 6070–6081.

[13] S.T. Kadhum, G.Y. Alkindi, T.M. Albayati, Remediation of phenolic wastewater implementing nano zerovalent iron as a granular third electrode in an electrochemical reactor, Int. J. Environ. Sci. Technol., 19 (2022) 1383–1392.

[14] C.-P. Leo, W.C. Cathie Lee, A.L. Ahmad, A.W. Mohammad, Polysulfone membranes blended with ZnO nanoparticles for reducing fouling by oleic acid, Sep. Purif. Technol., 89 (2012) 51–56.

[15] Y. He, J.M. Hong, Effect of nano-sized ZnO particle addition on PVDF ultrafiltration membrane performance, Adv. Mater. Res., 311–313 (2011) 1818–1821.

[16] A. Jalal Sadiq, K.M. Shabeeb, B.I. Khalil, Q.F. Alsalhy, Effect of embedding MWCNT-g-GO with PVC on the performance of PVC membranes for oily wastewater treatment, Chem. Eng. Commun., 207 (2020) 733–750.

[17] F.H. Al-Ani, Q.F. Alsalhy, R. Subhi Raheem, K.T. Rashid, A. Figoli, Experimental investigation of the effect of implanting TiO₂-NPs on PVC for long-term UF membrane performance to treat refinery wastewater, Membranes, 10 (2020) 77, doi: 10.3390/membranes10040077.

[18] D.M. Al-Ani, F.H. Al-Ani, Q.F. Alsalhy, S.S. Ibrahim, Preparation and characterization of ultrafiltration membranes from PPSU-PES polymer blend for dye removal, Chem. Eng. Commun., 208 (2021) 41–59.

[19] R.J. Kadhim, F.H. Al-Ani, Q.F. Alsalhy, MCM-41 mesoporous modified polyethersulfone nanofiltration membranes and their prospects for dyes removal, Int. J. Environ. Anal. Chem., (2021) 1–21, doi: 10.1080/03067319.2020.1865326.

[20] L. Shen, X. Bian, X. Lu, L. Shi, Z. Liu, L. Chen, Z. Hou, K.J.D. Fan, Preparation and characterization of ZnO/polyethersulfone (PES) hybrid membranes, Desalination, 293 (2012) 21–29.

[21] Y. Yang, H. Zhang, P. Wang, Q. Zheng, J. Li, The influence of nano-sized TiO₂ fillers on the morphologies and properties of PSf UF membrane, J. Membr. Sci., 288 (2007) 231–238.

[22] Q.F. Alsalhy, K.T. Rashid, S.S. Ibrahim, A.H. Ghanim, B. Van der Bruggen, P. Luis, M. Zablouk, Poly(vinylidene fluoride-co-hexafluropropylene) (PVDF-co-HFP) hollow fiber membranes prepared from PVDF-co-HFP/PEG-600Mw/DMAC solution for membrane distillation, J. Appl. Polym. Sci., 129 (2013) 3304–3313.

[23] M.J. Jamed, A.A. Alanezi, Q.F. Alsalhy, Effects of embedding functionalized multi-walled carbon nanotubes and alumina on the direct contact poly(vinylidene fluoride-cohexafluoropropylene) membrane distillation performance, Chem. Eng. Commun., 206 (2019) 1035–1057.

[24] A. Ahmad, A. Abdulkarim, S. Ismail, B.J.D. Ooi, Preparation and characterisation of PES-ZnO mixed matrix membranes for humic acid removal, Desal. Water Treat., 54 (2015) 3257–3268.

[25] J.-H. Kim, K.-H. Lee, Effect of PEG additive on membrane formation by phase inversion, J. Membr. Sci., 138 (1998) 153–163.

[26] L. Powell, N. Hilal, C.J.D. Wright, Atomic force microscopy study of the biofouling and mechanical properties of virgin and industrially fouled reverse osmosis membranes, Desalination, 404 (2017) 313–321.

[27] S. Shankar, L.-F. Wang, J.-W. Rhim, Incorporation of zinc oxide nanoparticles improved the mechanical, water vapor barrier, UV-light barrier, and antibacterial properties of PLA-based nanocomposite films, Mater. Sci. Eng., C, 93 (2018) 289–298.

[28] N.S. Ali, K.R. Kalash, A.N. Ahmed, T.M. Albayati, Performance of a solar photocatalysis reactor as pretreatment for wastewater

[29] via UV, UV/TiO₂, and UV/H₂O₂ to control membrane fouling, Sci. Rep., 12 (2022) 16782, doi: 10.1038/s41598-022-20984-0.

[29] J. Hong, Y.J.D. He, Effects of nano sized zinc oxide on the performance of PVDF microfiltration membranes, Desalination, 302 (2012) 71–79.

[30] S. Balta, A. Sotto, P. Luis, L. Benea, B. Van der Bruggen, J. Kim, A new outlook on membrane enhancement with nanoparticles: the alternative of ZnO, J. Membr. Sci., 389 (2012) 155–161.

[31] C.P. Leo, W.P. Cathie Lee, A.L. Ahmad, A.W. Mohammad, Polysulfone membranes blended with ZnO nanoparticles for reducing fouling by oleic acid, Sep. Purif. Technol., 89 (2012) 51–56.

[32] O.T. Mahlangu, R. Nackaertsb, J.M. Thwalac, B.B. Mambaa, A.R.D. Verliefde, Hydrophilic fouling-resistant GO-ZnO/PES membranes for wastewater reclamation, J. Membr. Sci., 524 (2017) 43–55.

[33] Q.F. Alsalhy, F.H. Al-Ani, A.E. Al-Najar, S.I.A. Jabuk, A study of the effect of embedding ZnO-NPs on PVC membrane performance use in actual hospital wastewater treatment by membrane bioreactor, Chem. Eng. Process. Process Intensif., 130 (2018) 262–274.

[34] A.L. Ahmad, J. Sugumaran, N.F. Shoparwe, Antifouling properties of PES membranes by blending with ZnO nanoparticles and NMP-acetone mixture as solvent, Membranes, 8 (2018) 131, doi: 10.3390/membranes8040131.

[35] A.M. Ali, K.T. Rashid, A.A. Yahya, H. Sh. Majdi, I.K. Salih, K. Yusoh, Q.F. Alsalhy, A.A. AbdulRazak, A. Figoli, Fabrication of gum arabic-graphene (GGA) modified polyphenylsulfone (PPSU) mixed matrix membranes: a systematic evaluation study for ultrafiltration (UF) applications, Membranes, 11 (2021) 542, doi: 10.3390/membranes11070542.

[36] A.K. Shukla, J. Alam, M. Alhoshan, L.A. Dass, M.R. Muthu-mareeswaran, Development of a nanocomposite ultrafiltration membrane based on polyphenylsulfone blended with graphene oxide, Sci. Rep., 7 (2017) 41976, doi: 10.1038/srep41976.

[37] K.C. Ho, Y.H. Teow, W.L. Ang, A.W. Mohammad, Novel GO/OMWCNTs mixed-matrix membrane with enhanced antifouling property for palm oil mill effluent treatment, Sep. Purif. Technol., 177 (2017) 337–349.

[38] H. Wu, B. Tang, P. Wu, Development of novel SiO₂–GO nanohybrid/polysulfone membrane with enhanced performance, J. Membr. Sci., 451 (2014) 94–102.

[39] Z. Shen, W. Chen, H. Xu, W. Yang, Q. Kong, A. Wang, M. Ding, J. Shang, Fabrication of a novel antifouling polysulfone membrane with in situ embedment of Mxene nanosheets, Int. J. Environ. Res. Public Health, 16 (2019) 4659, doi: 10.3390/ijerph16234659.

[40] R. Pang, X. Li, J. Li, Z. Lu, X. Sun, L. Wang, Preparation and characterization of ZrO₂/PES hybrid ultrafiltration membrane with uniform ZrO₂ nanoparticles, Desalination, 332 (2014) 60–66.

[41] D.A. Hussein Al-Timimi, Q.F. Alsalhy, A.A. AbdulRazak, Polyethersulfone/amine grafted silica nanoparticles mixed matrix membrane: a comparative study for mebeverine hydrochloride wastewater treatment, Alexandria Eng. J., 66 (2023) 167–190.

[42] R. Abdullah Reham, M. Shabeeb Kadhum, B. Alzubaydi Aseel, F. Alberto, C. Alessandra, D. Enrico, Q.F. Alsalhy, Chara-cterization of the efficiency of photo-catalytic ultrafiltration PES membrane modified with tungsten oxide in the removal of tinzaparin sodium, Eng. Technol. J., 40 (2022) 1621–1629.

[43] D.A. Hussein Al-Timimi, Q.F. Alsalhy, A.A. AbdulRazak, E. Drioli, Novel polyether sulfone/polyethylenimine grafted nano-silica nanocomposite membranes: Interaction mechanism and ultrafiltration performance, J. Membr. Sci., 659 (2022) 120784, doi: 10.1016/j.memsci.2022.120784.

[44] R.R. Abdullah, K.M. Shabeed, A.B. Alzubaydi, Q.F. Alsalhy, Novel photocatalytic polyether sulfone ultrafiltration (UF) membrane reinforced with oxygen-deficient tungsten oxide (WO₂.₈₉) for Congo red dye removal, Chem. Eng. Res. Des., 177 (2022) 526–540.

[45] F.H. Al-Ani, Q.F. Alsalhy, R.S. Raheem, K.T. Rashid, A. Figoli, Experimental investigation of the effect of implanting TiO₂-NPs on PVC for long-term UF membrane performance to treat refinery wastewater, Membranes, 10 (2020) 77.